HHS Public Access

Author manuscript

Neurotoxicology. Author manuscript; available in PMC 2019 July 22.

Published in final edited form as:

Neurotoxicology. 2017 September ; 62: 111–123. doi:10.1016/j.neuro.2017.06.003.

Chlorpyrifos and chlorpyrifos oxon impair the transport of membrane bound organelles in rat cortical axons

Jie Gao[1], **Sean X. Naughton**[1], **Wayne D. Beck**[1], **Caterina M. Hernandez**[1], **Guangyu Wu**[1], **Zhe Wei**[1], **Xiangkun Yang**[2], **Michael G. Bartlett**[2], **Alvin V. Terry Jr.**[1]

[1]Department of Pharmacology and Toxicology, Medical College of Georgia, Augusta University, Augusta, Georgia, 30912

[2]Department of Pharmaceutical and Biomedical Sciences, The University of Georgia College of Pharmacy, 250 W. Green Street, Athens, Georgia, 30602

Abstract

Chlorpyrifos (CPF) is an extensively used organophosphorus pesticide that has recently come under increasing scrutiny due to environmental health concerns particularly its association with neurodevelopmental defects. While the insecticidal actions and acute toxicity of CPF are attributed to its oxon metabolite (CPO) which potently inhibits the cholinergic enzyme acetylcholinesterase (AChE), there is significant evidence that CPF, CPO, and other organophosphates may affect a variety of neuronal targets and processes that are not directly related to AChE. Previously, in adult rat sciatic nerves *ex vivo* and postnatal neurons from rats in vitro we observed that CPF and CPO impaired the movements of vesicles and mitochondria in axons. Here, in embryonic neurons from rats in culture, we evaluated 24 hr exposures to CPF and CPO across picomolar to micromolar concentrations for effects on fast axonal transport of membrane bound organelles (MBOs) that contained the amyloid precursor protein (APP) tagged with the fluorescent marker, Dendra2 (APPDendra2). The most notable observations of this study were concentration-dependent decreases in the velocity and percentage of MBOs moving in the anterograde direction, an increase in the number of stationary MBOs, and an increased frequency of pauses associated with both CPF and CPO. These effects occurred at concentrations that did not significantly inhibit AChE activity, they were not blocked by cholinergic receptor antagonists, and they were not associated with compromised cell viability. These effects of CPF and CPO may be significant given the importance of axonal transport to neuronal development as well the function of fully developed neurons.

Corresponding Author: Alvin V. Terry Jr., Ph.D., Department of Pharmacology & Toxicology, 1120 15th Street, CB-3545, Augusta University, Augusta, Georgia 30912, Phone: 706-721-9462, Fax: 706-721-2347, aterry@auguta.edu.

Authorship Contributions

Participated in research design: Bartlett, Gao, Hernandez, Terry, Wu

Conducted experiments: Beck, Gao, Hernandez, Naughton, Wei, Yang

Performed data analysis: Gao, Hernandez, Naughton, Yang, Terry

Wrote or contributed to the writing of the manuscript: Bartlett, Gao, Hernandez, Naughton, Terry

Keywords

Pesticide; Organophosphate; Axonal Transport; Amyloid Precursor Protein; Neurodevelopment; Gulf War Illness

1. Introduction

Chlorpyrifos (O,O-diethyl O-[3,5,6, -trichloro-2-pyridyl] phosphorothionate) (CPF) is an organophosphorus pesticide used extensively worldwide especially in agricultural settings (see Solomon et al., 2014; Dow AgroSciences, 2017). It has a broad spectrum of insecticidal activity and other advantages such as a relatively short persistence in the environment after application and chemical characteristics that provide flexibility for use in multiple delivery systems (see Solomon et al., 2014; Dow AgroSciences, 2017). The insecticidal actions of CPF are attributed to its CPF oxon (CPO) metabolite which potently and irreversibly inhibits the enzyme acetylcholinesterase (AChE) leading to marked elevations of synaptic acetylcholine (Amitai et al., 1998; Ecobichon, 2001). While the oxidative desulfuration enzymes responsible for the conversion of phosphorothioates like CPF to their oxon metabolites are widely expressed in both insects and non-target organisms such as mammals and birds (Satoh and Gupta, 2010), the acute toxicity of CPF in mammals is considered “moderate” when compared to many other organophosphates (OPs). Despite this advantage, a variety of health concerns have arisen in the last several years over environmental exposures to CPF at levels below those associated with acute toxicity, most notably adverse neurodevelopmental effects in humans.

The potential of CPF to produce neurodevelopmental effects at relatively low doses is supported by human epidemiological data, prospective animal studies, and *in vitro* data. For example, epidemiologic studies have made associations between CPF in the maternal and/or umbilical cord blood (at concentrations as low as picogram/gram) and deleterious effects in the offspring including impairments of attention, intelligence quotient (IQ), and working memory (Rauh et al., 2006; Eskenazi et al., 2007 Horton et al., 2012; Rauh et al., 2012), abnormal motor development (Young et al., 2005; Engel et al. 2007; Zhang et al., 2014), and malformations of the cortex (Rauh et al., 2012). Likewise, prenatal exposures to CPF in rodents at doses that were not acutely toxic to the mother, have been shown to result in impairments of spatial reference and/or working memory (e.g., Icenogle et al., 2004, Billauer-Haimovitch et al., 2009; Mamczarz et al., 2016), alterations in locomotor activity (e.g., Levin et al., 2002; Ricceri et al., 2003) and morphological alterations of the hippocampus and prefrontal cortex (Chen et al., 2012). In PC12 cells in culture, 24 hours of exposure to CPF at a concentration 10-fold below the concentration that inhibited AChE activity (3.0 μM) impaired neurite outgrowth while CPO inhibited neurite outgrowth at 1.0 nM, a concentration that was close to the threshold for AChE inhibition in the same study (Das and Barone 1999). In embryonic rat sympathetic neurons in culture, exposure to CPF or CPO for 24 hr to concentrations well below those that inhibited AChE activity (nM and pM, respectively) decreased axonal outgrowth (Howard et al. 2005).

It is important to note, however, that some of the deleterious effects of CPF noted above, especially, the neurodevelopmental effects in humans are controversial (see Eaton et al., 2008; Li et al., 2012). In 2016, the United States Environmental Protection Agency (US EPA) proposed to revoke all tolerances for CPF (US EPA, 2016), based on concerns over neurodevelopmental effects in humans, an action that would have effectively removed CPF from the US agricultural market. This proposal was opposed by the USDA (see Kunickis, 2017) and moreover, it was not supported by an advisory board to the EPA which stated concerns over uncertainties in the available data particularly in establishing causal connections between such low levels of CPF and adverse neurodevelopmental effects in humans (EPA 2016). In 2017, the EPA reversed its proposal to revoke all tolerances to CPF, stating that the science addressing neurodevelopmental effects of CPF remains unresolved (EPA, 2017).

Despite the controversies described above, several of the *in vitro* studies suggest that targets other than AChE may also be important to the toxicology of both CPF and CPO. These studies are complemented by experiments of OPs across a variety of model systems which suggest that deleterious effects unrelated (or potentially additive) to AChE inhibition may include oxidative stress, impairments of mitochondrial function, neuroinflammation, and altered neurotrophin responses, etc. (Soltaninejad and Abdollahi, 2009; Banks and Lein, 2012; Terry, 2012). For several years our laboratory has been investigating the effects of OPs on fast axonal transport, a process that is essential to neuronal development as well as the maintenance and function of fully developed neurons (reviewed, Maday et al., 2014). Our early studies indicated that both anterograde and retrograde transport of vesicles in the sciatic nerves (*ex vivo*) was impaired in rats repeatedly exposed to doses of CPF that were below the threshold for acute toxicity. Moreover, the deficits in axonal transport were detected for up to 14 days after the last CPF injection indicating that the impairments were persistent (Terry et al., 2003; Terry et al., 2007). In a series of subsequent experiments in primary neuronal cultures from postnatal rats, we also observed morphological changes and impairments in the movement of mitochondria in axons associated with both CPF and CPO. Importantly, the changes in axonal transport of mitochondria occurred at concentrations of CPF and CPO that did not inhibit AChE activity (Middlemore-Risher et al., 2011). More recently, using manganese-enhanced magnetic resonance imaging (MEMRI) we observed that repeated exposures to doses of CPF that were below the threshold for acute toxicity led to prolonged impairments of axonal transport in the brains of living rats (Hernandez et al., 2015).

We have also recently developed a time-lapse imaging technique in embryonic rat cortical neurons for evaluating fast axonal transport of membrane bound organelles (MBOs) that contained the amyloid precursor protein (APP) tagged with the fluorescent marker, Dendra2 (APPDendra2). Using this technique, we evaluated the OP-nerve agent, diisopropylfluorophosphate (DFP) across a wide range of concentrations and observed DFP-related deficits in axonal transport associated with concentrations as low as 100 picomolar. Given the aforementioned controversies related to neurodevelopmental effects of CPF, the purpose of the experiments described here was 1) to evaluate CPF and CPO for effects on fast axonal transport using this embryonic culture model, and 2) to determine if an insecticide OP with very a different chemical structure from DFP (i.e., a phosphorothioate

and its oxon metabolite versus an alkylphosphate nerve agent), might have similar effects that are not directly related to AChE inhibition.

2. Materials and Methods

The methods used in this study were recently developed in our laboratory for measuring the trafficking of MBOs containing a transfected fluorophore-tagged amyloid precursor protein (APP) cDNA construct (Gao et al., 2016) in rat embryonic (cortical) neurons. The procedure is a modification of a previous method that was originally developed for rat spinal cord motor neurons (Magrane et al., 2012).

2.1 Chemicals

CPF (CAS number 2921–88-2) and CPO (CAS Number 5598–15-2) were obtained from ChemService, West Chester, PA (USA). CPF was dissolved in 0.5% dimethyl sulfoxide and used immediately. CPO was dissolved in methanol (80 mM) and stored at −80°C until needed.

Final toxin concentrations were prepared at 100-fold higher concentrations diluted from dimethyl sulfoxide (DMSO) and methanol stocks in Neurobasal media and the final concentrations of DMSO and methanol that were used in the cell cultures (for vehicle and OP exposures) were 0.01%. Atropine (ATR) and mecamylamine (MEC) were obtained from Sigma-Aldrich (St. Louis, MO, USA), stored as recommended by the source vendor and stock solutions were prepared in deionized water. ATR and MEC were prepared to use at 50.0 and 10.0 μM, respectively. All stock solutions were prepared at 100-fold higher concentrations in deionized water (≤ 5 (v/v) %, pH 7.0) within 15 minutes of the start of each 24-hour exposure period.

2.2 Embryonic cortical cultures

The cerebral cortices from E17–18 Sprague–Dawley rat embryos were extracted and cultured as described previously (Gao et al., 2014; 2016) under aseptic conditions. Timed pregnant rats were purchased from Harlan Sprague-Dawley, Inc. Indianapolis, IN and housed and maintained on a 12-hour light/dark cycle in a temperature-controlled room (25°C) with free access to food and water for at least 3 days prior to initiating cultures. All procedures used during this study were reviewed and approved by the Augusta University Institutional Animal Care and Use Committee and are consistent with the Association for Assessment and Accreditation of Laboratory Animal guidelines. Appropriate measures were taken to minimize pain or discomfort in accordance with the National Institute of Health Guide for the Care and Use of Laboratory Animals (National Research Council (U.S.) Committee for the Update of the Guide for the Care and Use of Laboratory Animals et al., 2011). Briefly, cortices were extracted and trypsinized (Trypsin-EDTA #25200, ThermoFisher Scientific Inc. Rockford, IL), then dissociated cellular material was seeded at a density of 5×10^5 cell/mL media onto poly-L-lysine (Sigma-Aldrich, St. Louis, MO) coated glass coverslips (25 mm) and 96-well plate (MTT cell proliferation assays). For AChE activity assays, cells were seeded at a density 1.1×10^6 cell/mL media on 10 cm petri dishes. Cultures were maintained at 37°C in a 5.0% CO_2 humidified atmosphere in

Neurobasal™ (#21103) supplemented with B27 (2.0 (v/v) %; #17504), Glutamax™ (0.5M, #35050) and Penicillin-Streptomycin (100 U/mL; #15140–122). All culture media materials were purchased from ThermoFisher Scientific Inc. Rockford, IL.

2.3 Cell transfection and treatments

All culture transfections were conducted at 37°C after 5–7 days *in vitro* (DIV) with APPDendra2-cDNA (Magrane et al., 2012) and Lipofectamine® 2000 (ThermoFisher Scientific Inc. Rockford, IL). All time-lapse imaging studies (see below) were conducted 24–36 hr post-transfection. Concentrations of CPF and CPO ranged from 0.1 to 10,000 nM and from 0.01 to 1000 nM, respectively and the OP or vehicle (VEH) exposure time was 24 hr. Prior to all live imaging experiments, culture media was exchanged with Neurobasal™ (#12348–017, ThermoFisher Scientific Inc. Rockford, IL) without phenol red.

2.4 Live imaging and Measurements of Axonal Transport

Transfected cells were located in primary cortical cultures using a Zeiss 780 LSM Inverted Confocal microscope connected digital microscope camera (AxioCam). Axons successfully transfected with APPDendra2 were identified by their fluorescence and morphological features (i.e., long neurites, constant thin diameter, no branching, perpendicular emergence from the cell body). Throughout the duration of the imaging session, cultures were maintained at 37°C under 5% CO_2 conditions within an environmental (i.e., heat and mixed gas controller) chamber. Once the APPDendra2 transfected neurons were localized (under 63X magnification, 1.42 numerical aperture), axons were video recorded for 3 min and frames were captured at a rate of one frame every 2 sec for a total of 90 frames (Zen, Carl Zeiss) to track the movements of dynamic particles and identify stationary particles. Using NIH ImageJ (http://rsb.info.nih.gov/ij/) with input/output and kymograph plug-ins, images were directly imported into ImagJ.. Briefly, kymographs (a graphic representation of a sample's position vs time) were generated to analyze the nature of APPDendra2 particle transport and directionality (i.e., anterograde, retrograde or stationary). Particle transport in the anterograde direction was identified by its movement away from the cell body and transport in the retrograde direction was identified by its movement towards the cell body. The distance traveled by each particle was measured in micrometers (μm) in linear segments of the axon. Individual particle velocities were measured in μm/sec during periods of sustained dynamic movement (i.e. ≥ 5 consecutive frames) and were calculated from the slope of a linear approximation of the trajectory. Stationary particles were identified by the absence of all movement throughout the 3 min video while pauses were defined as MBOs that were stationary for >5 consecutive frames, but not stationary for the entire recording. Additional measurements/calculations included the percentage of all particles that moved in the anterograde or retrograde direction or remained stationary, the number of APP-labeled MBOs/μm, the percentage of all particles that changed directions (reversals), the number of pauses per min of the video recording (Pause Frequencies) and the duration of the pauses (Pause Duration). Fig 1 provides an example of an APPDendra2 transfected neuron, a representative kymograph, and a series of video frames indicating movements of individual MBOs in the anterograde or retrograde direction.

2.5 Mecamylamine and atropine co-incubation experiments

The method described above for assessing axonal transport was also used to determine the effects of co-incubation of CPF and CPO with the muscarinic antagonist atropine or the nicotinic antagonist mecamylamine. Specifically, cortical neurons were co-incubated (for 24 hours) with either atropine (50 μM) or mecamylamine (10 μM) and a representative concentration of CPF and CPO shown to impair axonal transport (100 nM, 1.0 nM, respectively) in the first set of experiments (see results below). The representative concentrations of atropine and mecamylamine were based on previous *in vitro* studies (Middlemore-Risher et al., 2011; Gao et al., 2016).

2.6 Evaluation of cultured cell viability and toxicity

The concentration-dependent effects of CPF or CPO on cell viability (total number of viable cells) were assessed using a 96-well plate format Vybrant®MTT Cell Proliferation Assay kit (ThermoFisher Scientific Inc. Rockford, IL) according to the manufacturer's instructions. Cell viability measurements (DIV 7) are reported as the percentage of viable cells in comparison to the vehicle-treated cultures (i.e. control). In order to measure cellular toxicity associated with CPF or CPO, a Lactate Dehydrogenase Activity Assay Kit (Sigma-Aldrich® St. Louis, MO, USA. Lot# B9B270726V) was also used according to the manufacturer's instructions. Data for both cell viability and toxicity assays are expressed as percentage of output value (i.e. absorbance values) for CPF or CPO-exposed compared to the output value of vehicle-treated cell cultures (i.e. control).

2.6.1 Immunocytochemistry—Cultures (on 25 mm coverslips) were also processed to evaluate gross changes in neuronal morphology and cytoskeletal structure following 24 hr exposure to CPF (10 μM) or CPO (1.0 μM) compared to vehicle-treated controls (DIV 7). Immediately following CPF or CPO treatment, coverslips were washed 3 times in phosphate-buffered saline (PBS) sequentially decreasing in temperature from 37°C to 4°C, gradually fixed for 30 minutes in formalin (Thermo Fisher Scientific, Waltham, MA) (from 2.5 (v/v)% to 5 (v/v)% then a final 10 (v/v)%) and thoroughly washed with PBS. Briefly, coverslips were blocked in goat (MAP2A/2B) or donkey (DCX) serum-based blocking buffer, in percentage (v/v): 10 serum, 1.0 bovine serum albumin, 0.1 Triton X-100, 0.1 cold fish gelatin, and 0.05 Tween-20 for 30 minutes at room temperature then incubated in anti-MAP2A/2B (1:500) or DCX (1:400) overnight at 4°C. Following primary antibody incubation, coverslips were washed 3 times in PBS before incubation in goat anti-mouse (MAP2A/2B) or donkey anti-rabbit (DCX) (Jackson Immuno-Research, West Grove, PA) secondary antibody for 30min. Next, avidn-biotin amplification was employed, followed by incubation with streptavidin-conjugated AlexaFluor594 (Life Technologies/Molecular Probes, Eugene, OR). Coverslips were incubated for 2 hours at 25°C in Acti-stain™ 488 (Cytoskeleton, Denver, CO), a fluorophoreconjugated phalloidin, to assess cytoskeletal structure. All coverslips were mounted in DAPI-mounting media (Vectashield, Vector Laboratories, Burlingame, CA) to counterstain nuclei. Using confocal microscopy, all fluorescent staining was localized and identified under low magnification (< 40X) followed by image acquisition at 63X magnification (Zeiss 780 upright, Zeiss, Thornwood, NY). All images were captured as black and white digital images with pseudo-coloring added automatically by the Zen imaging software. Image processing (i.e. conversion between

formats, background noise reduction, etc.) was completed using ZEN (Zeiss), GIMP (http://gimp.org) 2.8, Adobe Photoshop and NIH ImageJ. All fluorescent images are presented as a z-projection from a 5-image z-stack. Phase Contrast images are presented as a single plane where neurites were in proper focus.

2.7 Preparation of cell lysates for AChE activity assays

Following transfections and/or chemical exposures, cultures were washed with PBS, transferred to a microtube after scraping from culture dishes into PBS (pH 8.0) containing Triton X-100 (final concentration = 1.0 (v/v) %) (PBS-TX100) and stored at −80°C. Samples were solubilized in PBS-TX100 at 4°C for 2 hrs with constant agitation. To remove cellular debris, samples were centrifuged at 13,400 $\times g$ for 1 minute at 4°C to clarify samples and collect the supernatant. Total protein for each supernatant collected was measured using detergent-compatible protein assay (Pierce Micro BCA™ Protein Assay Kit, ThermoFisher Scientific Inc. Rockford, IL) according to manufacturer's instructions.

2.8 Measurement of Acetylcholinesterase activity

Cell lysates (yielding a minimum of 8.0 ug/uL total protein) were assayed in duplicate to measure acetylcholinesterase (AChE) activity in samples after exposure to CPF or CPO. Effects of the OPs on purified eel AChE (CAS # 9000–81-1, Sigma-Aldrich, St. Louis, MO, USA), were also evaluated for comparison. AChE activity was assessed using the Ellman method with modifications to accommodate a 96-well microplate format at 25°C (Middlemore-Risher et al., 2011, Gao et al., 2016). The specific concentrations utilized for each chemical (Sigma-Aldrich, St. Louis, MO) in the reaction mixture (prepared in 1.0 mM sodium phosphate buffer (pH 7.0 ± 0.05) were as follows (in mM): 0.48 acetylthiocholine, 0.070 tetraisopropyl pyrophosphoramide (iso-OMPA, a butyrylcholinesterase inhibitor) and 0.52 mM 5,5′-dithiobis(2-nitrobenzoic acid). The formation of reaction product was monitored by measuring absorbance values at 412 nm every 2 minutes for 16 minutes (Mx synergy Microplate Spectrophotometer, BioTek Instruments Inc., Winooski, VT, USA). The rate of AChE activity was then calculated for each time point of measurement using the formula (change in absorbance/min)/ (1.36×10^4), then normalized to the intra-experiment vehicle-treated control.

2.9 Preparation of cells for analytical chemistry experiments

Neuronal cultures were also prepared for analytical chemistry experiments to determine if CPF was converted to CPO in the culture conditions. Cells were extracted and cultured from E18 embryos as described above. Cells were grown for 5–7 days in culture before harvest. Cultured cells, or Neurobasal Media were treated with concentrations of CPF ranging from 0.1 nM to 10 μM, CPO, 0.01 nM to 1.0 μM, or vehicle, for 1 or 24hrs at 37°C with 95% oxygen and 5% CO_2. After 1 or 24 hrs, treated media was collected and flash frozen on dry ice. Cells were rinsed twice with PBS, then scraped on ice and centrifuged at 13,400g for 1 minute at 4°C. Cell pellets were then flash frozen on dry ice. An additional 10 million cells were harvested and pelleted under similar conditions for calibration, along with 100 mL of untreated Neurobasal media.

2.10 Analytical Chemistry Experiments

In the experiments described here, the neuronal cell pellets, the media from the CPF and CPO-exposed cells, as well as media exposed to CPO and CPF without neurons present were also assayed by the LC-MS/MS method described below after 1 and 24 hr incubation periods. An additional experiment was conducted to determine if any CPO was present in the CPF crystalline powder obtained from ChemService and listed as 99.5% pure. For this experiment, CPF 1.0 mg/ml was dissolved in acetonitrile and compared to CPO 1.0 mg/ml (also dissolved in acetonitrile) and compared via the LC-MS/MS method described below.

2.10.1 Chemicals and reagents—Diisopropyl ether, LC-MS grade acetonitrile, methanol, water and formic acid were purchased from Sigma–Aldrich (St. Louis, MO).

2.10.2 Instrumentation—An Agilent 1100 binary pump HPLC system (Santa Clara, CA) connected with a Waters Micromass Quattro Micro triple quadrupole mass spectrometer with an ESI source (Milford, MA) was employed for LC–MS/MS analysis. Masslynx 4.0 software by Waters (Beverly, MA) was applied for data processing. A Labconco CentriVap Complete Vacuum Concentrator (Kansas City, MO) was utilized for sample evaporation.

2.10.3 LC-MS/MS conditions—A Zorbax Eclipse XDB-C8 (2.1×150 mm, 5 μm) column coupled with a Phenomenex SecurityGuard C-8 guard column (4.0 mm×2.0 mm) was applied for separation. The column temperature was maintained at 32 °C. The mobile phase A was 0.025% formic acid in water, and mobile phase B was acetonitrile. Analytes were separated using a gradient method, with a 0.3 mL/min flow rate, (time/minute, % mobile phase B): (0, 60), (2, 80), (2.01, 80), (5, 80), (6, 60), (10, 60). The injection volume was 15 μL, and the autosampler injection needle was washed with methanol after each injection. Samples were analyzed by the mass spectrometer in positive ion ESI mode for CPF and CPO, and in negative ion mode for TCP. Nitrogen was used as the desolvation gas at a flow rate of 500 L/hr. The desolvation temperature was 500 °C and the source temperature was 120 °C. Argon was used as the collision gas, and the collision cell pressure was 3.5×10^{-3} mbar. For TCP, the capillary voltage was −4 kV and the cone voltage was −22 V. For CPF and CPFO, the parameters were 3.5 kV and 28 V, respectively. The collision energy was 22 eV for CPF and 15 eV for CPO. A multiple reaction monitoring (MRM) function was applied for the detection of CPF and CPO. The ion transitions monitored were 352→200 for CPF and 336→280 for CPO. A selected ion recording (SIR) function for m/z = 198 was applied for the detection of TCP.

2.10.4 Sample preparation—Each 100 μL of cell culture media was extracted with 1.7 mL isopropyl ether. The mixture was vortexed for 10 min, then centrifuged at 7500 × g, at 5 °C for 10 min. 1.5 mL of supernatant was transferred and evaporated at 55 °C for 10 min to complete dryness in the vacuum concentrator. The sample was reconstituted with 100 μL of acetonitrile, sonicated, vortexed, and centrifuged at 7500 × g, 5 °C for 10 min. Eighty uL supernatant was transferred for injection into the LC-MS/MS system.

A cell pellet (1 million cells) was mixed with 1 mL methanol, vortexed and stored at −80 °C for 15 min. The cell lysate was centrifuged at 5 °C, 7500 × g for 10min, 0.9 mL of supernatant was transferred to a glass tube, mixed with 1 mL of acetonitrile, and evaporated at 55 °C for 45 min to complete dryness in the vacuum concentrator. The sample was reconstituted with 100 μL acetonitrile, vortexed, and centrifuged at 7500 × g, 5 °C for 10 min. 80 uL of supernatant was transferred for injection into the LCMS/MS system.

2.10.5 Calibration standards—The primary stock solutions were prepared at 1 mg/mL in acetonitrile for CPF, CPO and TCP, individually. Standard working solutions were obtained by serial dilution with acetonitrile, and their concentrations (ng/mL) for all analytes are in Table 1. A 10 μL standard working solution was spiked with 90 μL of blank cell culture media or 1 million cells, to make the corresponding calibration standards. Calibration curves were made with peak areas of analytes, with 1/x weighted linear regression. The concentration of each analyte was derived from the corresponding calibration curve.

2.11 Statistical Analyses

All statistical analyses were performed using SigmaPlot (Systat Software, San Jose, CA) Analysis of variance (ANOVA) was used to compare the concentration-dependent effects of chemical treatments to vehicle-treated controls and the method of Holm-Sidak was used to examine post hoc differences when indicated. Statistical significance was assessed using an alpha level of 0.05. Values depicted in the figures reflect the mean ± s.e.m. The number of independent experiments conducted for each drug evaluation and the number of replicates per drug concentration are indicated in the figure legends.

3. Results

3.1 APPDendra2 transfection and live imaging

Twenty-four hours following transfection, cultured neurons exhibited clear expression of APPDendra2 in the soma and axons (both of which were identified morphologically) (Fig 1A). For imaging, individual APPDendra2-labeled MBO’s in axons were identified under lower magnification as distinct (green fluorescent) structures with a circular or tubular shaped appearance (see the arrows in Figure 1A). At higher magnification (63X), definitive proximal and distal axonal regions of each axon were identified and corresponding kymographs (see Fig 1B for a sample) demonstrate that many MBOs were highly mobile, moving in both the anterograde and retrograde directions, while others remained stationary. The arrows in Fig 1C indicate individual MBOs moving along the axon at various stages in the anterograde and retrograde direction.

3.2 Effects of CPF and CPO on cell viability, neuronal morphology and cytoskeletal integrity

The effects of 24 hr incubation with CPF or CPO on cell viability across the same range of concentrations that were later evaluated in the axonal transport studies (see results below) were initially assessed using an MTT assay. As shown in Fig. 2A, at 24 hrs there were no significant effects of CPF at any of the concentrations that were evaluated. As a secondary

method for evaluating the effects of CPF on neuronal cell viability, an assay to measure lactate dehydrogenase (LDH) levels in the media was used. Compared to the control group treated with vehicle only, incubation with CPF did not significantly increase LDH release except at the highest concentration evaluated (10 μM) (Fig 2C). As shown in Fig. 2B in the MTT assay, there were slight, but significant ($p<0.05$) impairments in the viability of neurons exposed to the two highest concentrations of CPO that were evaluated (100 and 1000 nM). These two concentrations of CPO were also associated with increased LDH release (Fig 2D). Visual (qualitative) analyses of the histological images (actin, DCX, and MAP, see Fig 2E, F, and G, respectively) and phase contrast images (H) revealed no overt alterations in cellular morphology or structure after 24 hrs of exposure to CPF (10 μM) or CPO (1.0 μM).

3.3 CPF Impairs APP Axonal Transport

The results of the video and kymograph analyses of CPF on axonal transport of APP-labeled MBOs are provided in Fig 3 and Table 2. After 24 hrs of exposure to CPF, there was a significant ($p\leq0.05$) decrease in the velocity of APP transport in the anterograde direction associated with the three higher concentrations (100 nM–10μM) that were evaluated (Fig. 3A). The reduction in velocity was accompanied by a similar concentration-dependent decrease in the overall percentage of MBOs moving in the anterograde direction (Fig 3C) and an increase in the frequency of pauses (Table 2). Only the highest concentration of CPF (10 μM) was associated with a decrease in velocity of MBOs moving in the retrograde direction (Fig 3B) and no concentration of CPF affected the overall percentage of APP particles moving in the retrograde direction (Fig 3D). Interestingly, there was robust, concentration-dependent increase in the percentage of stationary MBOs (Fig 3E) associated with CPF (i.e., 5 of the 6 concentrations evaluated were associated with an increase). The insets below Fig 3A and 3B illustrate the segmental velocities of the MBOs associated with vehicle and a concentration of CPF (100 nM) that decreased velocity in the anterograde direction. The histograms indicate that in the case of anterograde transport, there was a wider range of velocities observed when compared to CPF 100 nM and that the highest percentage of particles were moving at a range of approximately 0.8–1.4 μm/sec compared to a range of approximately 0.7–1.0 μm/sec for the CPF-treated neurons. In the retrograde direction, the highest percentage of particles moved at a velocity of approximately 0.8 μm/sec, and this percentage did not appear to be altered by CPF 100 nM. There were no other CPF-related alterations observed in the video analyses which included the number of MBOs/μm, percent of reversals (MBOs changing direction), or in the pause durations (Table 2).

3.4 CPO Impairs APP Axonal Transport

The results of the video and kymograph analyses of CPO on axonal transport of APP-labeled MBOs are provided in Fig 4 and Table 2. After 24 hrs of exposure to CPO, there was a concentration-dependent decrease in the velocity of APP transport in both the anterograde and retrograde direction (Fig 4A and 4B respectively) and there was an increase in the frequency of pauses (Table 2). While concentrations of CPO as low as 0.1 nM resulted in ~20% decrease MBO velocity in the anterograde direction (Fig. 4A), the threshold for decreases in velocity in the retrograde direction was 10 nM (Fig. 4B). Exposure to several concentrations of CPO also resulted in a decrease in the overall percentage of particles

moving in the anterograde (but not retrograde) direction (Fig 4C and D respectively), and an increase in the overall percentage of stationary particles (Fig 4E). The insets below Fig 4A and 4B illustrate the segmental velocities of the MBOs associated with vehicle and a concentration of CPO (10 nM) that decreased velocity in the anterograde and retrograde directions. The histograms indicate that in the case of anterograde transport, the highest percentage of particles were moving at a range of approximately 1.2–1.4 μm/sec under vehicle conditions whereas, the highest percentage traveled around 0.6–0.8 μm/sec for the CPO-treated neurons. In the retrograde direction, the highest percentage of particles moved at a velocity of approximately 0.7–1.2 μm/sec in vehicle-treated neurons, whereas, the highest percentage traveled around 0.6–0.8 μm/sec for the CPO-treated neurons. There were no other CPF-related alterations observed in the video analyses which included the number of MBOs/μm, percentage of reversals, or in the pause durations (Table 2).

3.5 Muscarinic and nicotinic antagonists do not affect CPF or CPO-related impairments in APP axonal transport

Additional experiments were conducted to determine if either the muscarinic acetylcholine receptor antagonist atropine or the nicotinic acetylcholine receptor antagonist mecamylamine would affect the CPF or CPO-related impairments of axonal transport. Here a representative dose of CPF (100 nM) and CPO (1.0 nM) that was previously shown to inhibit anterograde axonal transport without affecting cell viability (in any of viability assessments) was evaluated in the absence or presence of cholinergic receptor antagonists. The results of these experiments are illustrated in Fig 5. The histograms on the left of Fig 5A indicate that neither atropine nor mecamylamine (when administered alone) affected anterograde axonal transport when compared to vehicle control. The histograms in the middle and to the right of Fig 5A show that the selected concentrations of CPF and CPO clearly impaired anterograde axonal transport and that these deficits persisted in the presence of either atropine or mecamylamine. Fig 5B illustrates the effects of the compounds and combinations on retrograde axonal transport. Neither atropine nor mecamylamine (when administered alone) significantly affected retrograde axonal transport when compared to vehicle control (left portion of Fig 5B). CPF (100 nM) was associated with modest, but statistically insignificant, impairments in retrograde axonal transport (an effect that was not altered by the cholinergic antagonists), and CPO 1.0 nM impaired retrograde transport, an effect that appeared to be reversed by atropine, but not mecamylamine.

3.6 Effects of CPF and CPO on AChE Activity

The effects of CPF and CPO on AChE activity *in vitro* are shown in Fig 6. In Fig 6A, the results of 24 hrs of exposure to CPF on neuronal cell lysates across the range of concentrations evaluated in the axonal transport studies indicate that the IC_{50} was greater than 10 μM and that the threshold for significant inhibition was likely around 1 μM. For comparison purposes, we also evaluated a wide range of concentrations of CPF in a well-established assay in our laboratory using purified eel AChE. Here (Fig 6B) the IC_{50} for CPF was also was greater than 10 μM. In Fig 6C, the results of 24 hr of exposure to CPO on neuronal cell lysates across the range of concentrations evaluated in the axonal transport studies indicate that the IC_{50} was approximately 26 nM. Similarly, in the purified eel AChE

preparation, the IC_{50} was approximately 10 nM. In both preparations, the threshold for significant inhibition appeared to be approximately 1.0 nM.

3.7 Conversion of CPF to CPO in culture

The final series of experiments were designed to determine if CPF conversion to CPO occurred in the cultures, thus indirectly contributing to the impairments of axonal transported described above. The results of these experiments are presented in Table 3. While the entire range of CPF concentrations that were tested in the axonal transport studies were also evaluated in the analytical experiments (0.1 nM to 10 μM), only concentrations of 100 nM and above were associated with quantifiable levels of CPF or its metabolites in the cultured neurons or media after 1 or 24 hr incubations. As indicated in Table 3, the CPF metabolites CPO and TCP were only detected in the media from CPF treated neurons (or from CPF-treated media without neurons present) after exposure to the highest (10 μM) concentration of CPF. In the case of the CPF-treated neurons very low (but quantifiable) levels of CPO were detected in association with 1.0 and 10.0 μM CPF while TCP was only detected in association with 10.0 μM CPF. CPO and TCP were not detected in cells or media after CPO was added (after 1 or 24 hours incubations). In the assessment of the CPO 1.0 mg/ml solution prepared from the CPF crystalline power that was used for making solutions for the culture experiments, the amount of CPO detected was approximately 0.05%.

4. Discussion

The major findings of this study can be summarized as follows: 1) 24 hours of exposure to the insecticide CPF or its oxon metabolite CPO resulted in a concentration-dependent decrease in the anterograde and (to a lesser extent) retrograde transport of MBOs in cortical axons from rats, 2) In some cases, the neuronal changes occurred at concentrations of CPF and CPO that did not significantly inhibit AChE activity, were below the threshold for neurotoxicity (as would be suggested by comprised cell viability or evidence of cytoskeletal damage), and they were not blocked by cholinergic receptor antagonists. The later observation further supports the argument that the CPF and CPO effects on axonal transport may not be directly related to AChE inhibition and the consequent elevations in synaptic levels of acetylcholine, since atropine and mecamylamine antagonize all known muscarinic and nicotinic receptor subtypes, respectively (see Wang et al., 2004; Lippiello et al., 2008). 3) Finally, the impairments in axonal transport associated with CPF did not appear to be a result of its conversion to CPO in significant amounts in the culture conditions, although CPO was detectable after exposures to the highest concentrations of CPF.

In some cases in the concentration-response analyses, the effect of the OPs at increasing the number of stationary MBOs appeared to occur at a different threshold concentration than the effects on velocity. While the basis of this effect is unclear, it could be explained by the fact that the OPs have at least some effect on both anterograde and retrograde directional movements (i.e., effects that could, collectively, contribute to the total number of stationary vesicles). Here it is also important to note that, as shown in the segmental velocity analysis, a range of velocities can account for the mean, thus a slowing of velocity from essentially a

mild effect to zero (a stationary MBO) would not necessarily be clearly reflected in a histogram representation of means.

The velocity of APP labeled MBO movements in cortical axons observed in this study under control conditions, ~0.4–2.0 μm/sec in the anterograde, and ~0.4–1.5 μm/sec in retrograde direction, fit well within the range (0.5–3.0μm/sec) that is generally considered as "fast axonal transport" (see review, Maday et al., 2014). APP has been documented in a number of previous studies to travel in neurons by fast axonal transport (Koo et al., 1990; Sisodia et al., 1993) in a process that is dependent on conventional kinesin (Amaratunga et al., 1993; Ferreira et al., 1993; Buxbaum et al., 1998). In fact, APP-positive vesicles are considered a canonical cargo of kinesin-1 motors (Kamal et al., 2000) transported primarily in the anterograde direction, although rapid retrograde motility has been observed (Falzone et al., 2009; Kaether et al., 2000) as we also report. The effects of the CPF oxon on anterograde axonal transport were similar to the results with DFP obtained in our previous study (Gao et al., 2016). These data indicate that organophosphorus compounds with considerably different chemical structures (alkylphosphate versus the oxon metabolite of a phosphorothioate) can exhibit quite similar profiles of fast, anterograde axonal transport impairments across a comparable range of low concentrations.

While the molecular mechanisms underlying the effects of CPF and CPO on axonal transport were not addressed in this study, previously published experiments would appear to implicate cytoskeletal proteins (e.g., tubulin) and/or motor proteins (e.g., kinesin) as potential targets of these OPs. For example, Prendergast et al., 2007 (utilizing a spectrophotometric method), demonstrated that CPO inhibited the polymerization of tubulin, and (utilizing organotypic slice cultures of rodent brain and histological methods) caused a marked decrease in the concentration of microtubule associated protein-2. Moreover, Lockridge and colleagues (utilizing atomic force microscopy), observed that CPO disrupted tubulin polymerization and further (utilizing mass spectrometry), that CPO covalently binds to tubulin, an effect that may explain the disruptions in tubulin polymerization (Grigoryan and Lockridge, 2009; Jiang et al., 2010). In the later study cited above (Jiang et al., 2010), CPO-labeled tubulin was found in the brains of mice (ex vivo) after repeated injections with CPF at a relatively low dose (3.0 mg/kg) that had only modest (statistically insignificant) effects on plasma AChE. Tubulin has also been identified as a target of DFP to affect microtubule dynamics and axonal transport. Specifically, DFP was recently shown to decrease tubulin acetylation to impair the axonal movements of mitochondria in both cultured rodent and human derived neurons. The effect of DFP was exacerbated by corticosterone or cortisol, in rat and human neurons, respectively (to mimic stress), and these negative effects were attenuated by tubacin, a drug that inhibits HDAC6, the tubulin deacetylase (Rao et al., 2017).

The hypothesis that CPF, CPO and other OPs negatively affect kinesin-driven axonal transport is supported by the results of *in vitro* microtubule motility assays conducted in our laboratory where an increase in the number of locomoting microtubules that detached from kinesin-coated glass was observed when kinesin was preincubated with CPF, CPO, or DFP (Gearhart et al., 2007). These data suggested that OPs might covalently modify kinesin and disrupt kinesin-microtubule interactions that are necessary for anterograde axonal transport.

This hypothesis is supported by the Grigoryan et al., 2009 study where covalent binding of FP-biotin (a biotin-tagged OP) to tyrosine in the human kinesin 3C motor domain was demonstrated.

Retrograde axonal transport was also impaired by CPF and CPO (albeit most evident at the higher concentrations that were evaluated) in the current study, indicating that in addition to kinesin, the retrograde motor protein dynein might also be affected by these OPs. To our knowledge, no studies have directly studied the effects of OPs on dynein-based retrograde axonal transport to date. Here it should be noted that, as opposed to our previous study with DFP (where concentrations as low as 0.1 nM impaired retrograde axonal transport), in the current study only the highest concentration of CPF (10 μM) and the three higher concentrations of CPO (ranging from 10 nM-1.0 μM) impaired retrograde axonal transport in the concentration-effect analyses. Here it is important to note that in the subsequent antagonist-reversal studies, we did detect impairments in retrograde impairments associated with the 1.0 nM concentration of CPO, indicating that this concentration may be at the threshold for impairment. These findings would appear to suggest that there may be some differences in how OPs of different structural classes affect dynein and/or other proteins that affect retrograde axonal transport (e.g., microtubule-binding proteins such as dynactin).

Alternative (or perhaps complimentary) targets of CPF and CPO that could contribute to our observations of axonal transport deficits are the variety protein kinases that are known to regulate axonal transport through direct phosphorylation of motors, adapter proteins, and cargoes. Among their variety of functions, several kinases are now known to regulate the transport of APP in axons and they include Akt, Erk1/2, GSK3β, and JNK (see review, Gibbs et al., 2015). As an important example, Erk1/2 phosphorylation of kinesin light chain-1 (KLC1) at Ser460 prevents binding of the motor to APP vesicles leading to a decrease in their anterograde transport (Vagnoniet al. 2011; 2012). The serine/threonine kinase Akt has been shown to regulate the directionality of fast axonal transport of APP through phosphorylation of the adapter protein htt (Colin t al., 2008). Our observations that the OPs did not affect the number of MBOs that reversed direction might argue that Akt levels (or kinase activity) were not markedly altered by these OPs at the concentrations that were evaluated.

Other potential mechanisms of the OP-related impairments include metabolic factors (e.g., superoxide formation and oxidative stress), and synthesis and packaging of APP. In our previous study of the effects of CPF and CPO in culture (using a similar range of concentrations) on mitochondrial transport and dynamics (Middlemore-Risher et al., 2011) we did not see any evidence of significant elevations in superoxide levels. Moreover, the observations in the current study that there were no alterations in the number of APP-containing MBOs per μm would argue against OP-related alterations in APP synthesis or packaging in vesicles.

Our previous observations of CPF and CPO-related impairments of mitochondrial movements (Middlemore-Risher et al., 2011) could also contribute to the impairments of APP (MBOs) transport observed in this study. Fast axonal transport of cargos moving along cytoskeletal networks is an ATP-dependent process that relies on proper mitochondrial

placement. Without the appropriate placement of mitochondria, ATP availability and buffering of intracellular calcium is compromised, resulting in the impairment of a variety of processes (including axonal transport) (Chang and Reynolds, 2006a and b).

As noted above, the final phase of experiments conducted in this study were designed to determine if the effects of CPF on axonal transport might have occurred indirectly as a result of the conversion of CPF to CPO by the cultured neurons and/or the culture media. In mammals, (primarily in the liver), the conversion of CPF to CPO occurs as a result of the oxidative desulfuration of CPF, a reaction catalyzed by cytochrome P-450 (CYP) enzymes. However, most CYP subfamilies are also present in the brain and they can metabolize molecules of exogenous origin (albeit at a much lower rate) (see Miksys and Tyndale, 2002 for review). While our cultures conditions (using Neurobasal™ media) were developed to minimize the proliferation of glial cells, some glia were always present and, importantly, both neurons and glia are known to express CYP enzymes. The induction of CYPs in glial cells by xenobiotics is thought play a role in protecting neurons from environmental insults (see Tripathi et al., 2013), however, in the context of this study, the potential CYP-related conversion of CPF to CPO by glia cells would not likely be protective. Thus, an interesting question (for potential future study) is whether the deleterious effects of CPF observed in the current study would be higher or lower in pure neuronal cultures. The conversion of CPF to CPO has also been demonstrated in chlorinated tap water (see Wu and Laird, 2003), thus given the variety of electrolytes present in our culture media, this was a concern.

Despite the concerns discussed above about CPF metabolism or degradation, the results indicated that CPO and TCP were only detected in association with the highest (μM) concentrations of CPF that were added to the culture media (either when neuron/glia were present or absent). Given that CPF altered anterograde axonal transport at concentrations as low as 100 nM, these effects seem unlikely to be fully explained by conversion of CPF to CPO or TCP in culture. However, there are some limitations to this interpretation that should be considered. As indicated in Table 3, the levels of CPF detected in the media after one hour were significantly lower than the molar concentrations added (i.e., decreased by approximately 33–52%) and they were further reduced at 24 hrs (i.e., decreased by approximately 80–88%). The source of this decrease in concentration is unclear, it is possible that CPF may have adsorbed to the plastic or was potentially volatilized. Moreover, CPO is known to spontaneously decompose in aqueous media relatively rapidly (see Kaushik et al., 2007) making its accurate quantitation from cultures difficult, especially over long incubation times.

In conclusion, the results of the experiments described in this study support the argument that CPF-related impairments of fast anterograde axonal transport could be a contributing factor to a variety of deleterious effects that have been attributed to this OP. The transport of organelles and macromolecules (e.g., mitochondria, receptor proteins, growth factors) from the cell body toward synaptic terminals is essential both during the development of post-mitotic neurons as well as for the normal maintenance and function of developed neurons (reviewed, Duncan and Goldstein 2006; Maday et al., 2014). While this study was conducted in embryonic neurons in culture and, thus, most relevant to the reported neurodevelopmental effects of CPF, our afformentioned findings of CPF-related axonal transport deficits in adult

rats (*ex vivo* and *in vivo*, see Terry et al, 2007; Hernandez et al., 2015) suggest that this effect may occur irrespective of age. These observations could, therefore, have important ramifications for environmental exposures to OPs in agriculture as well as diseases such as gulf war illness (GWI), where exposures to OP-based insecticides and nerve agent-OPs (following the destruction of an Iraqi munitions storage complex at Khamisiyah, Iraq, in March 1991) have been implicated (RAC, 2014). Moreover, there is a small but growing body of literature to suggest that OP exposure may even represent a potential risk factor for Alzheimer's disease (AD) and other neurodegenerative disorders (Hancock et al., 2008; Hayden et al., 2010; Zaganas et al., 2013). Interestingly, impairments in axonal transport have been implicated in the pathology of AD as well as a wide variety of other neurological illnesses (see Stokin and Goldstein, 2006 for review).

Acknowledgments

The authors thank Ms. Ashley Davis for administrative assistance in preparing this article.

The work described in this manuscript was supported by the National Institute of Environmental Health Sciences [R01ES012241] (Terry), the Congressionally Directed Medical Research Programs (CDMRP), specifically, the Gulf War Illness Research Program (GWIRP), grant number W81XWH-12–1-0536 (Terry), and the National Institute of General Medical Sciences [R01GM118915] (Wu).

References

Amaratunga A, Morin PJ, Kosik KS, Fine RE. (1993) Inhibition of kinesin synthesis and rapid anterograde axonal transport in vivo by an antisense oligonucleotide. J Biol Chem. 15;268(23): 17427–30. [PubMed: 7688725]

Amitai G, Moorad D, Adani R, Doctor BP. (1998) Inhibition of acetylcholinesterase and butyrylcholinesterase by chlorpyrifos-oxon. Biochem Pharmacol. 1;56(3):293–9. [PubMed: 9744565]

Banks CN, Lein PJ. (2012) A review of experimental evidence linking neurotoxic organophosphorus compounds and inflammation. Neurotoxicology. 33(3):575–84. Review. [PubMed: 22342984]

Billauer-Haimovitch H, Slotkin TA, Dotan S, Langford R, Pinkas A, & Yanai J (2009). Reversal of chlorpyrifos neurobehavioral teratogenicity in mice by nicotine administration and neural stem cell transplantation. Behavioural Brain Research, 205(2), 499–504. [PubMed: 19682500]

Buxbaum JD, Thinakaran G, Koliatsos V, O'Callahan J, Slunt HH, Price DL, Sisodia SS. (1998) Alzheimer amyloid protein precursor in the rat hippocampus: transport and processing through the perforant path. J Neurosci. 18:9629–9637. [PubMed: 9822724]

Chang DT, Reynolds IJ. (2006a) Mitochondrial trafficking and morphology in healthy and injured neurons. Prog Neurobiol. 80(5):241–68. Review. [PubMed: 17188795]

Chang DT, Reynolds IJ. (2006b) Differences in mitochondrial movement and morphology in young and mature primary cortical neurons in culture. Neuroscience. 25;141(2):727–36. [PubMed: 16797853]

Chen XP, Chen WZ, Wang FS, Liu JX. (2012) Selective cognitive impairments are related to selective hippocampus and prefrontal cortex deficits after prenatal chlorpyrifos exposure. Brain Res. 20;1474:19–28. [PubMed: 22842080]

Colin E Zala D, Liot G, Rangone H, Borrell-Pagès M, Li XJ, Saudou F, Humbert S. (2008) Huntingtin phosphorylation acts as a molecular switch for anterograde/retrograde transport in neurons. EMBO J. 27, 2124–2134. [PubMed: 18615096]

Das KP, Barone S Jr. (1999) Neuronal differentiation in PC12 cells is inhibited by chlorpyrifos and its metabolites: is acetylcholinesterase inhibition the site of action? Toxicol Appl Pharmacol.1;160(3): 217–30. [PubMed: 10544056]

Dow AgroSciences (2017). Chlorpyrifos in Agriculture. Dow AgrosSciences LLC, Indianapolis, IN.

Duncan JE and Goldstein LS (2006) The genetics of axonal transport and axonal transport disorders. PLoS Genet 2:e124 [PubMed: 17009871]

Eaton DL, Daroff RB, Autrup H, Bridges J, Buffler P, Costa LG, Coyle J, McKhann G, Mobley WC, Nadel L, Neubert D, Schulte-Hermann R, Spencer PS. (2008) Review of the toxicology of chlorpyrifos with an emphasis on human exposure and neurodevelopment. Crit Rev Toxicol. 38 Suppl 2:1–125.

Ecobichon DJ (2001) Pesticide use in developing countries. Toxicology 160:27–33. [PubMed: 11246121]

Engel SM, Berkowitz GS, Barr DB, Teitelbaum SL, Siskind J, Meisel SJ, Wetmur JG, Wolff MS. (2007) Prenatal organophosphate metabolite and organochlorine levels and performance on the Brazelton Neonatal Behavioral Assessment Scale in a multiethnic pregnancy cohort. Am J Epidemiol. 165:1397–1404. [PubMed: 17406008]

Eskenazi B, Marks AR, Bradman A, Harley K, Barr DB, Johnson C, Morga N, Jewell NP. (2007) Organophosphate pesticide exposure and neurodevelopment in young Mexican-American children. Environ Health Perspect.115(5):792–8. [PubMed: 17520070]

Falzone TL, Stokin GB, Lillo C, Rodrigues EM, Westerman EL, Williams DS, Goldstein LS. (2009) Axonal stress kinase activation and tau misbehavior induced by kinesin-1 transport defects. J Neurosci. 29:5758–5767. [PubMed: 19420244]

Ferreira A, Caceres A, Kosik KS. (1993) Intraneuronal compartments of the amyloid precursor protein. J Neurosci;13:3112–3123. [PubMed: 8331388]

Gao J, Naughton SX, Wulff H, Singh V, Beck WD, Magrane J, Thomas B, Kaidery NA, Hernandez CM, Terry AV Jr. (2016) Diisopropylfluorophosphate Impairs the Transport of Membrane-Bound Organelles in Rat Cortical Axons. J Pharmacol Exp Ther.356(3):645–55. [PubMed: 26718240]

Gao J, Adam B-L, and Terry AV Jr. (2014) Evaluation of nicotine and cotinine analogs as potential neuroprotective agents for Alzheimer's disease. Bioorg Med Chem Lett 24:1472–1478. [PubMed: 24581918]

Gearhart DA, Sickles DW, Buccafusco JJ, Prendergast MA, Terry AV Jr. (2007) Chlorpyrifos, chlorpyrifos-oxon, and diisopropylfluorophosphate inhibit kinesin-dependent microtubule motility. Toxicol Appl Pharmacol. 1;218(1):20–9. [PubMed: 17123561]

Gibbs KL, Greensmith L, Schiavo G. (2015). Regulation of Axonal Transport by Protein Kinases. Trends Biochem Sci. 40(10):597–610. [PubMed: 26410600]

Grigoryan H, Lockridge O. (2009) Nanoimages show disruption of tubulin polymerization by chlorpyrifos oxon: implications for neurotoxicity Toxicol Appl Pharmacol 240(2):143–8. [PubMed: 19631231]

Grigoryan H, Li B, Anderson EK, Xue W, Nachon F, Lockridge O, and Schopfer LM (2009) Covalent binding of the organophosphorus agent FP-biotin to tyrosine in eight proteins that have no active site serine. Chem Biol Interact 180:492–498. [PubMed: 19539807]

Hancock DB, Martin ER, Mayhew GM, Stajich JM, Jewett R, Stacy MA, Scott BL, Vance JM, and Scott WK (2008) Pesticide exposure and risk of Parkinson's disease: a family-based case-control study. BMC Neurol 8:6. [PubMed: 18373838]

Hayden KM, Norton MC, Darcey D, Ostbye T, Zandi PP, Breitner JC, Welsh-Bohmer KA, and Cache County Study Investigators (2010) Occupational exposure to pesticides increases the risk of incident AD: the Cache County study. Neurology 74:1524–1530. [PubMed: 20458069]

Hernandez CM, Beck WD, Naughton SX, Poddar I, Adam BL, Yanasak N, Middleton C, Terry AV Jr. (2015) Repeated exposure to chlorpyrifos leads to prolonged impairments of axonal transport in the living rodent brain. Neurotoxicology.47:17–26. [PubMed: 25614231]

Horton MK, Kahn LG, Perera F, Barr DB, Rauh V. (2012) Does the home environment and the sex of the child modify the adverse effects of prenatal exposure to chlorpyrifos on child working memory? Neurotoxicol Teratol. 34(5):534–41. [PubMed: 22824009]

Howard AS, Bucelli R, Jett DA, Bruun D, Yang D, Lein PJ. (2005) Chlorpyrifos exerts opposing effects on axonal and dendritic growth in primary neuronal cultures. Toxicol Appl Pharmacol 207(2):112–24. [PubMed: 16102564]

Icenogle LM, Christopher NC, Blackwelder WP, Caldwell DP, Qiao D, Seidler FJ, Slotkin TA, Levin ED. (2004) Behavioral alterations in adolescent and adult rats caused by a brief subtoxic exposure to chlorpyrifos during neurulation. Neurotoxicol Teratol 26(1):95–101. [PubMed: 15001218]

Jiang W, Duysen EG, Hansen H, Shlyakhtenko L, Schopfer LM, and Lockridge O (2010) Mice treated with chlorpyrifos or chlorpyrifos oxon have organophosphorylated tubulin in the brain and disrupted microtubule structures, suggesting a role for tubulin in neurotoxicity associated with exposure to organophosphorus agents. Toxicol Sci 115:183–193 [PubMed: 20142434]

Kaether C, Skehel P, Dotti CG. Axonal membrane proteins are transported in distinct carriers: a two-color video microscopy study in cultured hippocampal neurons. Mol Biol Cell. 2000;11:1213–1224. [PubMed: 10749925]

Kamal A, Stokin GB, Yang Z, Xia CH, Goldstein LS. Axonal transport of amyloid precursor protein is mediated by direct binding to the kinesin light chain subunit of kinesin-I. Neuron. 2000;28:449–459. [PubMed: 11144355]

Kaushik R, Rosenfeld CA, Sultatos LG. (2007) Concentration-dependent interactions of the organophosphates chlorpyrifos oxon and methyl paraoxon with human recombinant acetylcholinesterase. Toxicol Appl Pharmacol. 1;221(2):243–50. [PubMed: 17467020]

Koo EH, Sisodia SS, Archer DR, Martin LJ, Weidemann A, Beyreuther K, Fischer P, Masters CL, Price DL (1990) Precursor of amyloid protein in Alzheimer disease undergoes fast anterograde axonal transport. Proc Nat Acad Sci USA 87:1561–1565. [PubMed: 1689489]

Kunickis Sheryl H. (2017) “To Jack E. Housenger.” USDA Comments on Chlorpyrifos Risk Assessment” 81 FR 81049, Docket ID EPA-HQ-OPP-2015–0653. 1 17, 2017.

Levin ED, Addy N, Baruah A, Elias A, Christopher NC, Seidler FJ, Slotkin TA (2002) Prenatal chlorpyrifos exposure in rats causes persistent behavioral alterations. Neurotoxicol Teratol 24(6): 733–41. [PubMed: 12460655]

Li AA, Lowe KA, McIntosh LJ, Mink PJ. (2012) Evaluation of epidemiology and animal data for risk assessment: chlorpyrifos developmental neurobehavioral outcomes. J Toxicol Environ Health B Crit Rev.15(2):109–84. Review. [PubMed: 22401178]

Lippiello PM, Beaver JS, Gatto GJ, James JW, Jordan KG, Traina VM, Xie J, Bencherif M. (2008). TC-5214 (S-(+)-mecamylamine): a neuronal nicotinic receptor modulator with antidepressant activity. CNS Neurosci Ther. 14(4):266–77. [PubMed: 19040552]

Maday S, Twelvetrees AE, Moughamian AJ, Holzbaur EL. (2014) Axonal transport: cargo-specific mechanisms of motility and regulation. Neuron. 22;84(2):292–309. Review. [PubMed: 25374356]

Magrané J, Sahawneh MA, Przedborski S, Estévez AG, and Manfredi G. (2012) Mitochondrial dynamics and bioenergetic dysfunction is associated with synaptic alterations in mutant SOD1 motor neurons. J Neurosci 32:229–242. [PubMed: 22219285]

Mamczarz J, Pescrille JD, Gavrushenko L, Burke RD, Fawcett WP, DeTolla LJ Jr, Chen H, Pereira EF, Albuquerque EX. (2016) Spatial learning impairment in prepubertal guinea pigs prenatally exposed to the organophosphorus pesticide chlorpyrifos: Toxicological implications. Neurotoxicology. 2016 9;56:17–28. [PubMed: 27296654]

Middlemore-Risher ML, Adam BL, Lambert NA, Terry AV Jr. (2011) Effects of chlorpyrifos and chlorpyrifos-oxon on the dynamics and movement of mitochondria in rat cortical neurons. J Pharmacol Exp Ther. 339(2):341–9. [PubMed: 21799050]

Miksys SL, Tyndale RF. (2002) Drug-metabolizing cytochrome P450s in the brain. J Psychiatry Neurosci. 27(6):406–15. Review. [PubMed: 12491573]

National Research Council (U.S.). Committee for the Update of the Guide for the Care and Use of Laboratory Animals, Institute for Laboratory Animal Research (U.S.) and National Academies Press (U.S.) (2011) Guide for the care and use of laboratory animals. National Academies Press, Washington, D.C.

Prendergast MA, Self RL, Smith KJ, Ghayoumi L, Mullins MM, Butler TR, Buccafusco JJ, Gearhart DA, and Terry AV Jr. (2007) Microtubule-associated targets in chlorpyrifos oxon hippocampal neurotoxicity. Neuroscience 146:330–339. [PubMed: 17321052]

Rao AN, Patil A, Brodnik ZD, Qiang L, España RA, Sullivan KA, Black MM, Baas PW. Pharmacologically increasing microtubule acetylation corrects stress-exacerbated effects of organophosphates on neurons. Traffic 2017 (in press) 5 4. doi: 10.1111/tra.12489.

Rauh VA, Garfinkel R, Perera FP, Andrews HF, Hoepner L, Barr DB, Whitehead R, Tang D, Whyatt RW (2006). Impact of prenatal chlorpyrifos exposure on neurodevelopment in the first 3 years of life among inner-city children. Pediatrics. 118(6):e1845–59. [PubMed: 17116700]

Rauh VA, Perera FP, Horton MK, Whyatt RM, Bansal R, Hao X, Liu J, Barr DB, Slotkin TA, Peterson BS. (2012) Brain anomalies in children exposed prenatally to a common organophosphate pesticide. Proc Natl Acad Sci U S A. 15;109(20):7871–6. [PubMed: 22547821]

Research Advisory Committee on Gulf War Veterans' Illnesses (RAC) (2014) Gulf War Illness and the Health of Gulf War Veterans: Research Update and Recommendations, 2009–2013. U.S. Department of Veterans Affairs, Washington, DC http://www.va.gov/RACGWVI/RACReport2014Final.pdf

Ricceri L, Markina N, Valanzano A, Fortuna S, Cometa MF, Meneguz A, Calamandrei G. (2003) Developmental exposure to chlorpyrifos alters reactivity to environmental and social cues in adolescent mice Toxicol Appl Pharmacol. 15;191(3):189–201. [PubMed: 13678652]

Satoh T, Gupta RC (eds). (2010) Anti- cholinesterase Pesticides: Metabolism, Neurotoxicity, and. Epidemiology. Wiley, Hoboken, NJ, 237–65.

Sisodia SS, Koo EH, Hoffman PN, Perry G, Price DL. (1993) Identification and transport of full-length amyloid precursor proteins in rat peripheral nervous system. J Neurosci. 13(7):3136–42. [PubMed: 8331390]

Solomon KR, Williams WM, Mackay D, Purdy J, Giddings JM, Giesy JP. (2014) Properties and uses of chlorpyrifos in the United States. Rev Environ Contam Toxicol. 231:13–34. [PubMed: 24723132]

Soltaninejad K, Abdollahi M. (2009) Current opinion on the science of organophosphate pesticides and toxic stress: a systematic review. Med Sci Monit. 15(3):RA75–90. [PubMed: 19247260]

Stokin GB and Goldstein LS (2006) Axonal transport and Alzheimer's disease. Annu Rev Biochem 75:607–627. [PubMed: 16756504]

Terry AV Jr, Stone JD, Buccafusco JJ, Sickles DW, Sood A, Prendergast MA. (2003) Repeated exposures to subthreshold doses of chlorpyrifos in rats: hippocampal damage, impaired axonal transport, and deficits in spatial learning. J Pharmacol Exp Ther. 305(1):375–84. [PubMed: 12649392]

Terry AV Jr, Gearhart DA, Beck WD Jr, Truan JN, Middlemore ML, Williamson LN, Bartlett MG, Prendergast MA, Sickles DW, Buccafusco JJ. (2007) Chronic, intermittent exposure to chlorpyrifos in rats: protracted effects on axonal transport, neurotrophin receptors, cholinergic markers, and information processing. J Pharmacol Exp Ther. 322(3):1117–28. [PubMed: 17548533]

Terry AV, Beck WD, Warner S, Vandenhuerk L, Callahan PM. (2012) Chronic impairments in spatial learning and memory in rats previously exposed to chlorpyrfos or diisopropylfluorophosphate. Neurotoxicol Teratol 34(1):1–8. [PubMed: 22024239]

Tripathi VK, Kumar V, Singh AK, Kashyap MP, Jahan S, Kumar D, Lohani M (2013). Differences in the expression and sensitivity of cultured rat brain neuronal and glial cells toward the monocrotophos. Toxicol Int 20:177–185. [PubMed: 24082512]

US EPA (2016). Proposal to Revoke Chlorpyrifos Food Residue Tolerances. https://archive.epa.gov/epa/ingredients-used-pesticide-products/proposal-revoke-chlorpyrifos-food-residue-tolerances.html.

US EPA (2017). Order Denying Petition to Revoke All Tolerances for the Pesticide Chlorpyrifos. https://www.epa.gov/ingredients-used-pesticide-products/order-denying-petition-revoke-all-tolerances-pesticide.

Vagnoni A Rodriguez L, Manser C, De Vos KJ, Miller CC. (2011) Phosphorylation of kinesin light chain 1 at serine 460 modulates binding and trafficking of calsyntenin-1. J. Cell Sci 124, 1032–1042. [PubMed: 21385839]

Vagnoni A Perkinton MS, Gray EH, Francis PT, Noble W, Miller CC. (2012) Calsyntenin-1 mediates axonal transport of the amyloid precursor protein and regulates Ab production. Hum. Mol. Genet 21, 2845–2854. [PubMed: 22434822]

Wang Z, Shi H, Wang H. (2004) Functional M3 muscarinic acetylcholine receptors in mammalian hearts Br J Pharmacol. 142(3): 395–408. [PubMed: 15148264]

Wu J, Laird DA. (2003) Abiotic transformation of chlorpyrifos to chlorpyrifos oxon in chlorinated water. Environ Toxicol Chem.22(2):261–4. [PubMed: 12558155]

Young JG, Eskenazi B, Gladstone EA, Bradman A, Pedersen L, Johnson C, Barr DB, Furlong CE, Holland NT. (2005) Association between in utero organophosphate pesticide exposure and abnormal reflexes in neonates. Neurotoxicology. 2005 3;26(2):199–209. [PubMed: 15713341]

Zaganas I, Kapetanaki S, Mastorodemos V, Kanavouras K, Colosio C, Wilks MF, and Tsatsakis AM (2013) Linking pesticide exposure and dementia: what is the evidence? Toxicology 307:3–11 [PubMed: 23416173]

Zhang Y, Han S, Liang D, et al., 2014 Prenatal exposure to organophosphate pesticides and neurobehavioral development of neonates: a birth cohort study in Shenyang, China. PLOS ONE 9 (2), e88491. [PubMed: 24551109]

Research Highlights

- Chlorpyrifos and Chlorpyrifos oxon impair axonal transport in embryonic neurons
- The transport deficits were not blocked by muscarinic or nicotinic antagonists
- Deficits occurred at concentrations below the threshold for cholinesterase inhibition

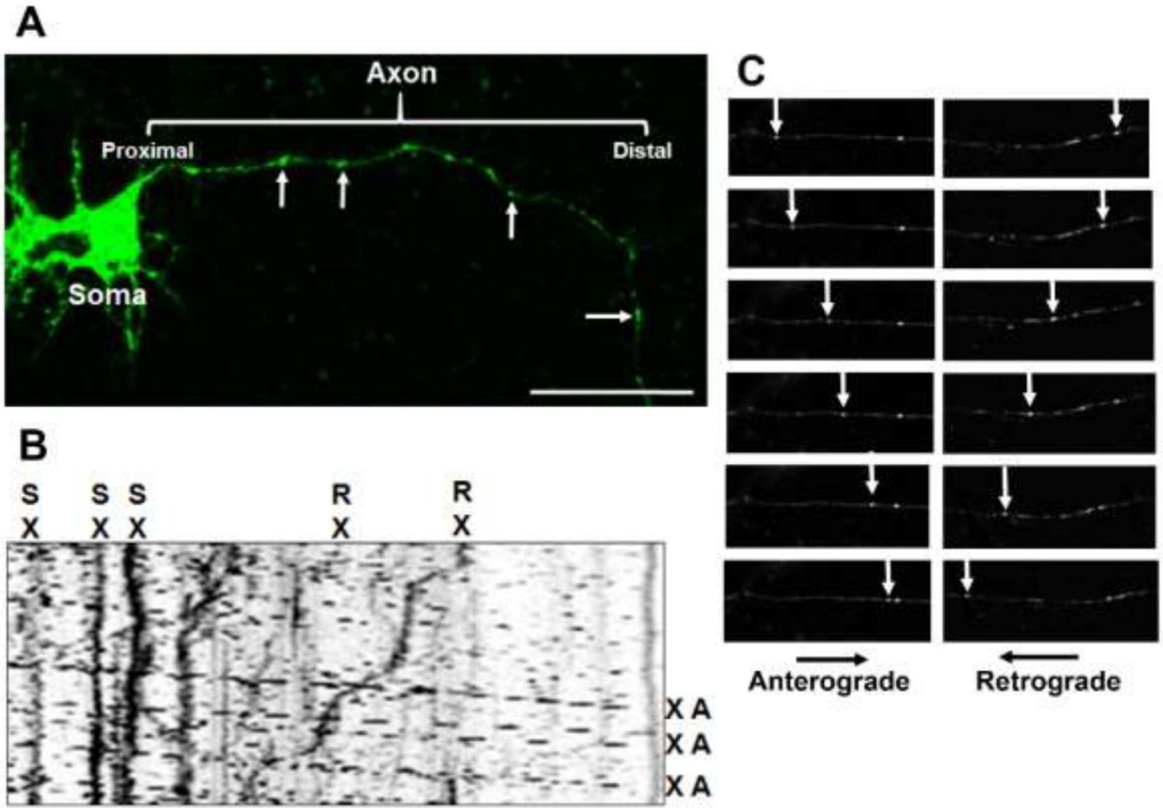

Fig 1. Methods for assessing the effects of chlorpyrifos (CPF) and chlorpyrifos oxon (CPO) on axonal transport in vitro.

(A) Representative image demonstrating successful transfection of APPDendra2 in rat primary cortical neurons. Green fluorescent membrane bound organelles (MBOs) in the axon are indicated by the arrows. (B) Kymograph recorded for 3 min with frames captured at a rate of one frame every 2 sec generated from APPDendra2-labeled MBOs after treatment with CPO. MBOs are categorized in one of three ways: anterograde (A), retrograde (R) or stationary (S). Velocity information was obtained from the slope of the lines. Scale bar = 20 μm. (C) Representative frames illustrating MBOs moving at various stages in the anterograde and retrograde directions (see arrows).

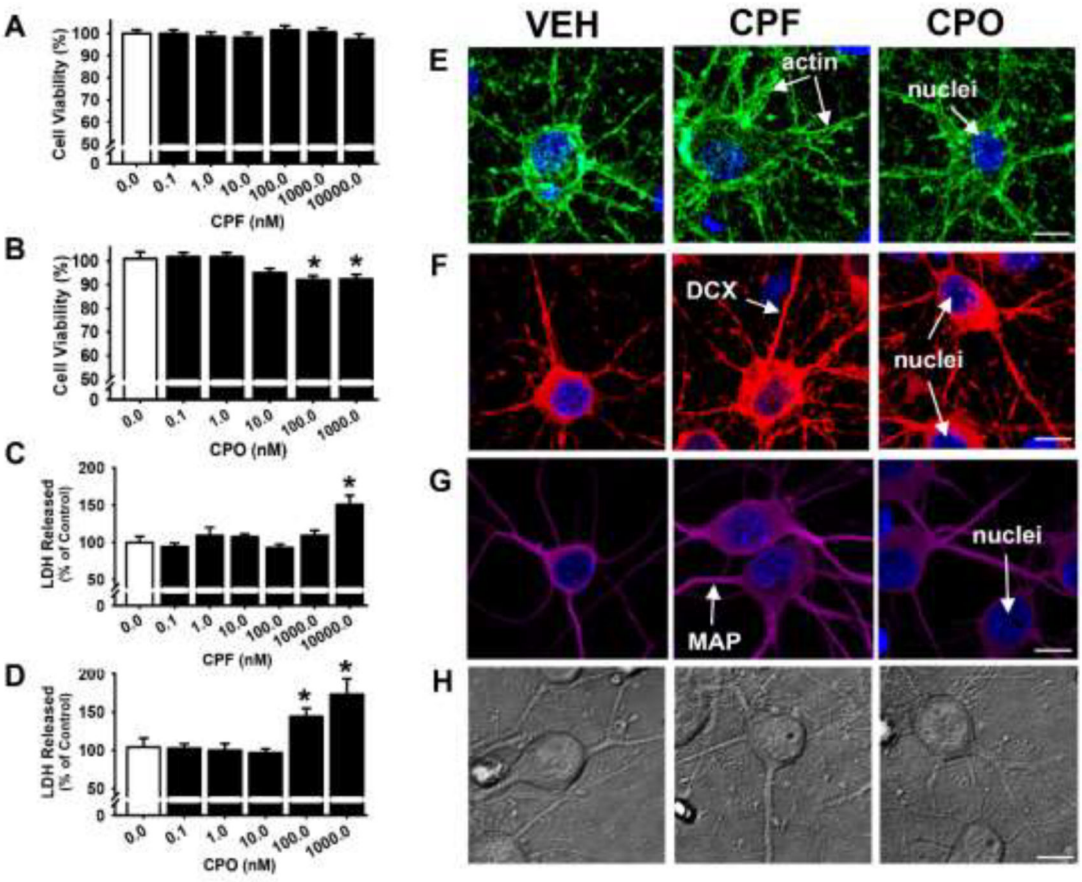

Fig 2. Only high concentrations of chlorpyrifos (CPF) and chlorpyrifos oxon (CPO) are associated with impairments in cell viability.

Following 24 hours of exposure to CPF (A,B) or CPO (C,D), cell viability was measured by both MTT colorimetric and LDH release assays, presented as the percentage of cell survival or release, respectively, compared to vehicle-treated controls (DIV 7). Each bar represents the mean ± s.e.m. (n = 2–3 independent experiments), "*", $p < 0.05$ compared vehicle control conditions. (E-G) Representative immunocytochemistry images of fluorophore-conjugated actin (Acti-stain 488, green), DCX (red), MAP2A/2B (magenta) and nuclei (blue), and (H) phase contrast images were obtained for visual comparisons of cellular morphology and structure after 24 hours exposure to 10 μM CPF or CPO 1.0 μM (DIV 7). Scale Bar = 10 μm.

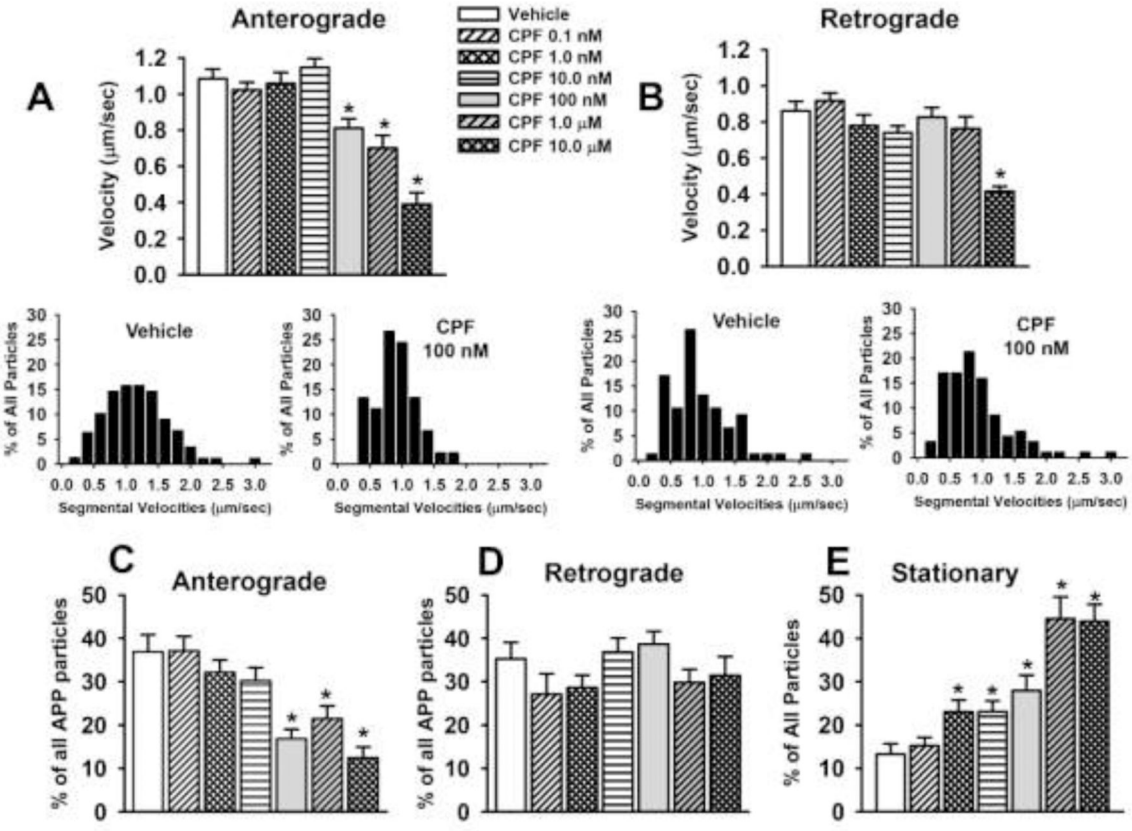

Fig 3. Chlorpyrifos (CPF) exposure for 24 hr impairs axonal transport in primary cortical neurons.

(A) Velocities of APP containing membrane bound organelles (MBOs) in the anterograde direction. (B) Velocities of APP containing MBOs in the retrograde direction. The insets below Fig 3A and 3B illustrate the segmental velocities of the MBOs associated with vehicle and a concentration of CPF (100 nM) that decreased velocity in the anterograde direction. (C-F) percentage of all particles that moved in the anterograde or retrograde direction or remained stationary. Each bar represents the mean ± s.e.m of measurements from 10–16 individual neurons (n=10–16) obtained in 3–4 separate experiments with 4–5 replicates/ concentration. The total number of moving MBOs that were analyzed in these experiments was 1080. * = significantly different than vehicle control conditions.

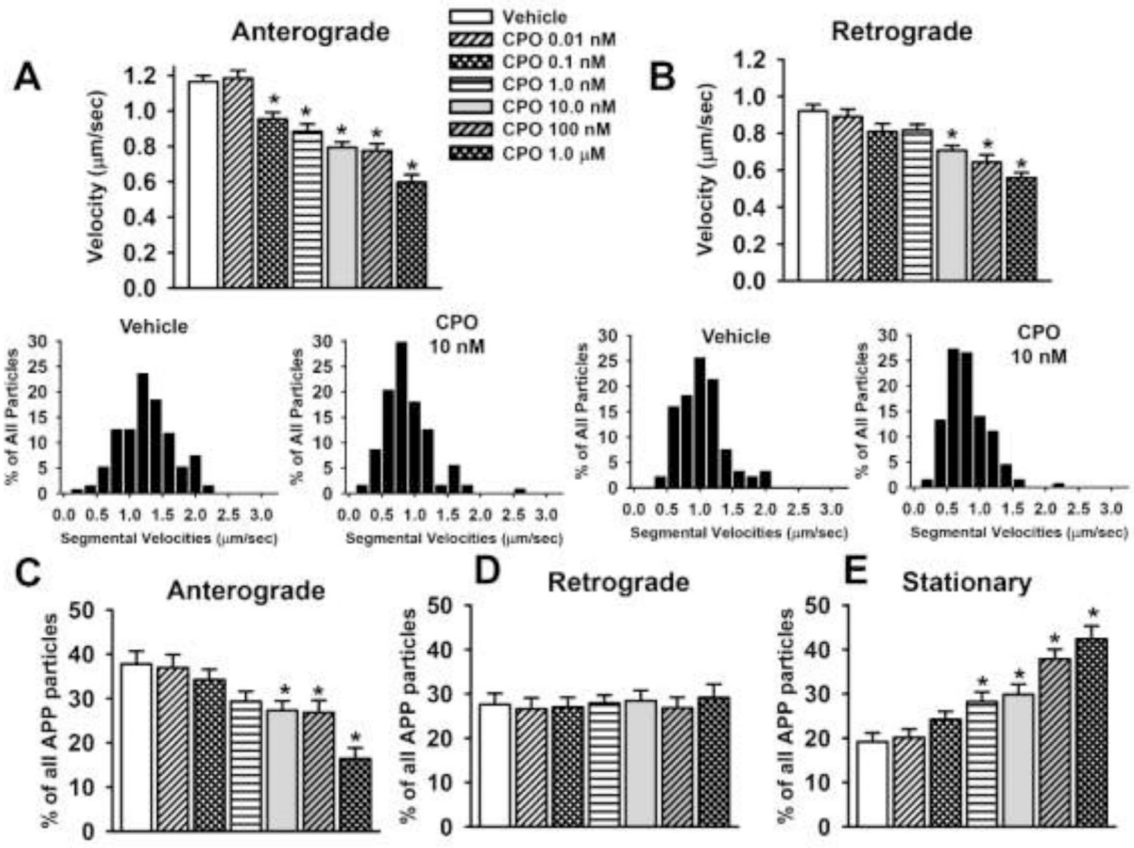

Fig 4. Chlorpyrifos oxon (CPO) exposure for 24 hr impairs axonal transport in primary cortical neurons.

(A) Velocities of APP containing membrane bound organelles (MBOs) in the anterograde direction. (B) Velocities of APP containing MBOs in the retrograde direction. The insets below Fig 3A and 3B illustrate the segmental velocities of the MBOs associated with vehicle and a concentration of CPO (1.0 nM) that decreased velocity in the anterograde direction. (C-F) percentage of all particles that moved in the anterograde or retrograde direction or remained stationary. Each bar represents the mean ± s.e.m of measurements from 12–20 individual neurons (n=12–20) obtained in 3–4 separate experiments with 4–5 replicates/ concentration. The total number of moving MBOs that were analyzed in these experiments was 1464. * = significantly different than vehicle control conditions.

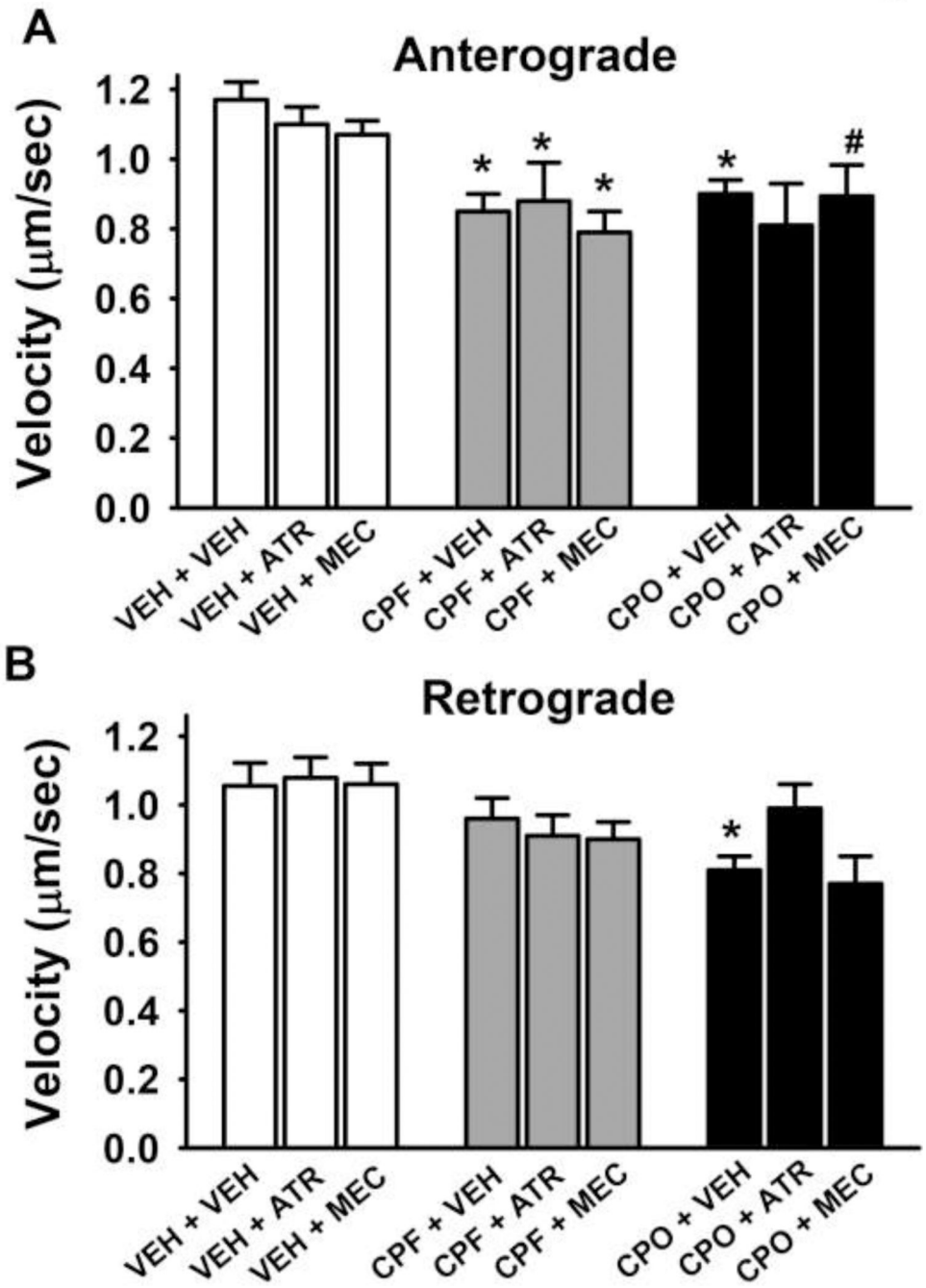

Fig 5. Muscarinic and nicotinic antagonists do not affect chlorpyrifos (CPF) or chlorpyrifos oxon (CPO)-related impairments in anterograde axonal transport in primary cortical neurons after 24hr of exposure.

(A) Velocities of APP containing membrane bound organelles (MBOs) moving in the anterograde direction. (B) Velocities of APP containing MBOs moving in the retrograde direction. Each bar represents the mean ± s.e.m of measurements from 10–20 individual neurons (n=10–20) obtained in 2 separate experiments with 4–5 replicates/concentration. The total number of moving MBOs that were analyzed in these experiments was 1108. ATR = atropine, MEC = mecamylamine. The concentrations of the compounds were as follows:

ATR 50 μM, MEC 10 μM, CPF 100 nM, CPO 1.0 nM. * = significantly different than vehicle control conditions. # = $p<0.06$ versus control.

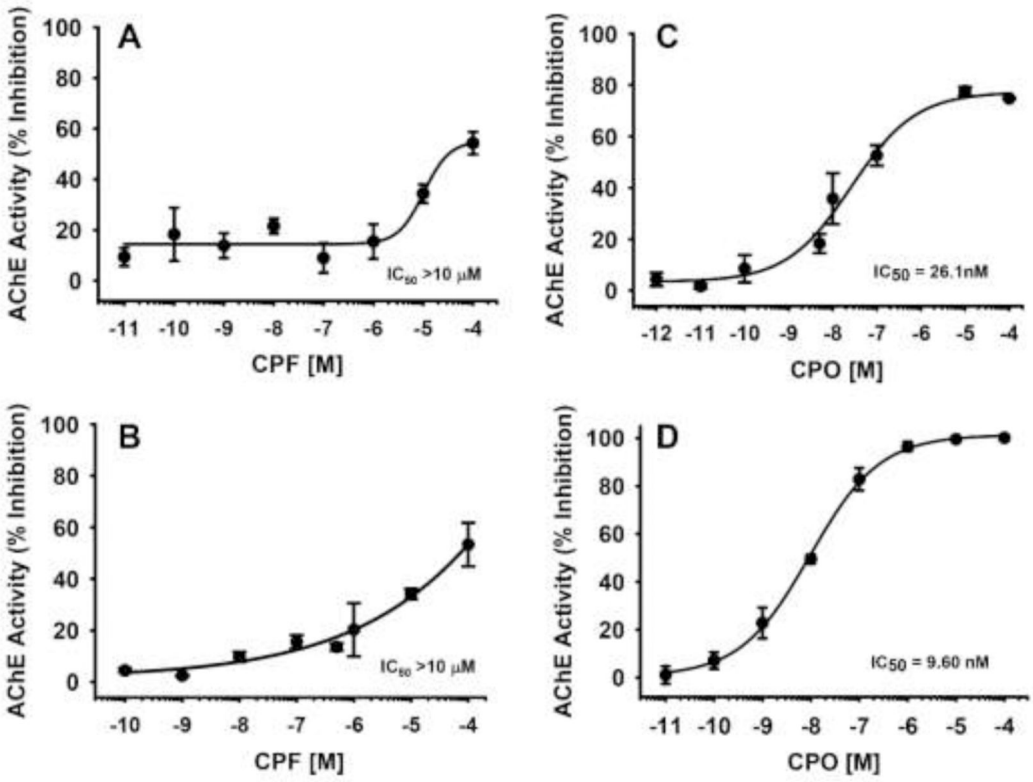

Fig 6. Effects of chlorpyrifos (CPF) and chlorpyrifos oxon (CPO) on acetylcholinesterase (AChE) activity in vitro.

(A) The effects of 24 hr of exposure to CPF on AChE activity in neuronal cell lysates across the range of concentrations evaluated in the axonal transport studies. (B) Effects of CPF across a wide range of concentrations on purified eel AChE. (C) The effects of 24 hr of exposure to CPO on AChE activity in neuronal cell lysates across the range of concentrations evaluated in the axonal transport studies. (D) Effects of CPF across a wide range of concentrations on purified eel AChE. Each symbol represents the mean ± s.e.m from 2 independent experiments and 3 replicates per concentration.

Table 1:

Concentrations (ng/mL) of analytes in standard working solutions.

Standard Working Solution	CPF	CPO	TCP
A	5000	200	20000
B	2500	100	10000
C	1250	50	5000
D	500	20	2000
E	250	10	1000
F	125	5	500
G	50	2	200

Table 2.

Additional Axonal Transport-Related Measurements

Compound	Concentration	APP Particles	Reversals	Pause Frequency	Pause Duration
	nM	# of MBOs/mm	% of All Particles	# pauses/min	sec
Chlorpyrifos	0.0	0.19 ± 0.01	22.28 ± 2.70	0.30 ± 0.06	38.99 ± 6.10
	0.1	0.17 ± 0.01	23.28 ± 2.49	0.31 ± 0.06	30.83 ± 3.70
	1.0	0.23 ± 0.02	23.59 ± 2.21	0.41 ± 0.09	37.41 ± 4.16
	10.0	0.24 ± 0.02	15.48 ± 1.65	0.46 ± 0.06	44.62 ± 4.20
	100.0	0.17 ± 0.01	13.94 ± 2.32	0.62 ± 0.09 *	47.40 ± 4.77
	1000.0	0.19 ± 0.01	18.26 ± 2.82	0.64 ± 0.11 *	43.58 ± 3.41
	10000.0	0.23 ± 0.02	19.29 ± 3.08	0.76 ± 0.11 *	41.00 ± 5.02
Chlorpyrifos Oxon	0.0	0.21 ± 0.01	15.42 ± 2.12	0.32 ± 0.06	37.38 ± 4.47
	0.01	0.23 ± 0.02	16.36 ± 1.77	0.56 ± 0.08	34.61 ± 3.30
	0.1	0.19 ± 0.01	14.58 ± 2.57	0.57 ± 0.07 *	37.41 ± 4.16
	1.0	0.26 ± 0.01	14.45 ± 1.75	0.78 ± 0.08 *	34.61 ± 3.09
	10.0	0.24 ± 0.01	14.36 ± 1.59	0.81 ± 0.11 *	33.92 ± 2.40
	100.0	0.23 ± 0.01	8.54 ± 1.40	1.29 ± 0.10	34.16 ± 2.88
	1000.0	0.24 ± 0.02	12.10 ± 2.39	1.03 ± 0.10 *	35.46 ± 3.54

Each value represents the mean ± s.e.m obtained from 12–20 individual neurons from 3–4 separate experiments and 4–5 replicates/concentration

* = significantly ($p<0.05$) different from vehicle control (0.0 concentration) conditions.

Table 3.

Conversion of CPF to CPO and TCP in Culture

Exposure Conditions	CPF Added	CPF Measured	CPO Measured	TCP Measured
		Mean ± S.E.M	Mean ± S.E.M	Mean ± S.E.M
CPF Exposed Neurons (1 hr)	100 nM	2.22 ± 0.11 ng	ND	<LLOQ
	1000 nM	25.05 ± 0.57 ng	<LLOQ	<LLOQ
	10000 nM	180.57 ± 0.84 ng	0.01 ± 0.00 ng	2.69 ± 0.02 ng
CPF Exposed Neurons (24 hr)	100 nM	0.47 ± 0.00 ng	ND	ND
	1000 nM	3.59 ± 0.11 ng	0.01 ± 0.00 ng	ND
	10000 nM	39.95 ± 2.66 ng	0.03 ± 0.00 ng	0.59 ± 0.13 ng
Media From CPF Exposed Neurons (1 hr)	100 nM	67.77 ± 2.70 nM	ND	<LLOQ
	1000 nM	611.36 ± 32.04 nM	<LLOQ	<LLOQ
	10000 nM	4759.43 ± 70.72 nM	0.57 ± 0.02 nM	<LLOQ
Media From CPF Exposed Neurons (24 hr)	100 nM	13.68 ± 0.23 nM	ND	ND
	1000 nM	118.01 ± 7.26 nM	<LLOQ	ND
	10000 nM	2053.49 ± 68.24 nM	0.39 ± 0.06 nM	1224.68 ± 52.39 nM
CPF Exposed Media (no neurons present)	100 nM	ND	ND	ND
(24 hr)	1000 nM	191.62 ± 26.42 nM	ND	ND
	10000 nM	2449.84 ± 111.67 nM	0.57 ± 0.06 nM	829.37 ± 113.13 nM

CPF = chlorpyrifos; CPO = chlorpyrifos oxon; TCP = 3,5,6-trichloropyridinol; ND = Not Detected; LLOQ = lower limit of quantification

Each value represents the mean ± s.e.m obtained from 4–6 replicants per toxin concentration obtained in 2 separate experiments